

On the relation between radial alignment of dark matter subhalos and host mass in cosmological simulations

Alexander Knebe¹, Nadya Draganova¹, Chris Power², Gustavo Yepes³,
Yehuda Hoffman⁴, Stefan Gottlöber¹, and Brad K. Gibson⁵

¹*Astrophysical Institute Potsdam, An der Sternwarte 16, Germany*

²*Department of Physics & Astronomy, University of Leicester, University Road, Leicester LE1 7RH, UK*

³*Grupo de Astrofísica, Universidad Autónoma de Madrid, Madrid E-28049, Spain*

⁴*Racah Institute of Physics, Hebrew University, Jerusalem 91904, Israel*

⁵*Centre for Astrophysics, University of Central Lancashire, Preston PR1 2HE, UK*

Submitted Version ...

ABSTRACT

We explore the dependence of the radial alignment of subhalos on the mass of the host halo they orbit in. As the effect is seen on a broad range of scales including massive clusters as well as galactic systems it only appears natural to explore this phenomenon by means of cosmological simulations covering the same range in masses. We have 25 well resolved host dark matter halos at our disposal ranging from $10^{15}h^{-1}M_{\odot}$ down to $10^{12}h^{-1}M_{\odot}$ each consisting of order of a couple of million particles within the virial radius. We observe that subhalos tend to be more spherical than isolated objects. Both the distributions of sphericity and triaxiality of subhalos are Gaussian distributed with peak values of $\langle s \rangle \approx 0.80$ and $\langle T \rangle \approx 0.56$, irrespective of host mass. Interestingly we note that the radial alignment is independent of host halo mass and the distribution of $\cos \theta$ (i.e. the angle between the major axis E_a of each subhalo and the radius vector of the subhalo in the reference frame of the host) is well fitted by a simple power law $P(\cos \theta) \propto \cos^4 \theta$ with the same fitting parameters for all host halos.

Key words: galaxies: evolution – galaxies: haloes – cosmology: theory – cosmology: dark matter – methods: N -body simulations

1 INTRODUCTION

The concordance of multitude of recent cosmological studies has demonstrated that we appear to live in a spatially flat, Λ -dominated cold dark matter (Λ CDM) universe (cf. Spergel et al. 2007). During the past decade simulation codes and computer hardware have advanced to such a stage where it has been possible to resolve in detail the formation of dark matter halos and their subhalo populations in a cosmological context (e.g. Klypin et al. 1999). These results, coupled with the simultaneous increase in observational data (e.g. 2 degree Field galaxy redshift survey (2dFGRS), Colless (2003); Sloan Digital Sky Survey (SDSS), Adelman-McCarthy (2007)), has opened up a whole new window on the concordance cosmogony in the field that has become known as “near-field cosmology” (Freeman & Bland-Hawthorn 2002).

One property of the galaxy population that has been measured is the spatial distribution of satellites about their primaries. Some evidence suggests that this is anisotropic, with satellites clustering about the major axis of the primary. An anisotropic spatial distribution has been measured

in various observational data sets (e.g. Zaritsky et al. 1997; Sales & Lambas 2004; Brainerd 2005; Yang et al. 2006; Bailin et al. 2007, please note that its interpretation continues to be a matter of debate though); a similar result is obtained for the distribution of subhalos in simulations of cosmological dark matter halos (e.g. Knebe et al. 2004; Zentner et al. 2005; Libeskind et al. 2005), as well as following from theoretical modelling (Lee et al. 2005).

Another property of the satellite population that has been measured is the radial alignment of their primary axes with respect to the host. The first evidence for this effect was reported for the Coma cluster, where it was observed that the projected major axes of cluster members preferentially align with the direction to the cluster centre (Hawley & Peebles 1975; Thompson 1976). Such a correlation between satellite elongation and radius vector has further been confirmed by statistical analysis of the SDSS data (Pereira & Kuhn 2005; Agustsson & Brainerd 2006; Faltenbacher et al. 2007; Wang et al. 2007). However, we also acknowledge that Bernstein & Norberg (2002) did not find such a signal in the 2dFGRS. The radial alignment of subhalo shapes towards the centre of their host has

Table 1. Details about the hosts and their subhalo populations. $N_{p,\text{host}}$ gives the number of particles in the host while M_{vir} measures its mass (in $10^{14}h^{-1}M_{\odot}$) and the mass R_{host} its virial radii (in $h^{-1}\text{kpc}$). The last two columns give the number of satellites in excess of $N_p > 200$ and $N_p > 200, b/a < 0.9$, respectively. These (sub-)samples of all identified subhalos comply with the criteria to reliably measure a) shape (S) and b) radial alignment (RA). Please refer to the text for further details.

| host | $N_{p,\text{host}}$ | M_{host} | R_{host} | $N_{\text{sub}}^{\text{S}}$ | $N_{\text{sub}}^{\text{RA}}$ |
|------|---------------------|-------------------|-------------------|-----------------------------|------------------------------|
| MC1 | 2608898 | 13.05 | 2288 | 217 | 115 |
| MC2 | 2531440 | 10.90 | 2155 | 165 | 79 |
| MC3 | 2275913 | 15.37 | 2417 | 137 | 77 |
| C1 | 1764131 | 2.87 | 1355 | 85 | 33 |
| C2 | 864068 | 1.41 | 1067 | 61 | 33 |
| C3 | 654169 | 1.06 | 973 | 27 | 11 |
| C4 | 859385 | 1.40 | 1061 | 38 | 12 |
| C5 | 725694 | 1.18 | 1008 | 34 | 10 |
| C6 | 869614 | 1.41 | 1065 | 46 | 17 |
| C7 | 1752783 | 2.85 | 1347 | 90 | 30 |
| C8 | 1868533 | 3.05 | 1379 | 127 | 56 |
| C9 | 1755223 | 1.25 | 1047 | 112 | 53 |
| C10 | 1918720 | 1.01 | 976 | 91 | 54 |
| C11 | 1918359 | 1.59 | 1133 | 117 | 68 |
| C12 | 894831 | 1.82 | 1187 | 80 | 34 |
| G1 | 1094732 | 0.178 | 547 | 59 | 46 |
| G2 | 1093805 | 0.178 | 547 | 90 | 46 |
| G3 | 1083392 | 0.176 | 545 | 97 | 48 |
| G4 | 1010659 | 0.164 | 532 | 48 | 32 |
| G5 | 971312 | 0.158 | 525 | 42 | 34 |
| MW1 | 2226368 | 0.014 | 227 | 100 | 28 |
| MW2 | 1734197 | 0.019 | 250 | 81 | 66 |
| MW3 | 1535393 | 0.017 | 242 | 86 | 49 |
| MW4 | 1384565 | 0.014 | 228 | 73 | 40 |
| MW5 | 1155977 | 0.022 | 265 | 71 | 25 |

also been measured for the subhalo population in cosmological simulations (Kuhlen et al. 2007; Faltenbacher et al. 2007; Pereira et al. 2007). We note that this effect was predicted by Ciotti & Dutta (1994), who used simulations to argue that cluster galaxies were influenced by the tidal field of the host cluster tidal field.

In this *Letter* we provide evidence that the radial alignment of subhalos in cosmological simulations does not depend on the mass of their host dark matter halo. In addition, we show that subhalo triaxialities and shapes follow a Gaussian distribution, which again does not depend on the mass of the host.

2 THE DATA

2.1 The Host Halos

We use a set of 25 high-resolution cosmological (zoom) simulations of individual dark matter host halos. Three of these runs (MC1-3) represent massive galaxy cluster of $M \approx 10^{15}h^{-1}M_{\odot}$. We have twelve cluster-sized objects (C1-12) with $M \approx 10^{14}h^{-1}M_{\odot}$, there are five group-sized systems (G1-5) with $M \approx 10^{13}h^{-1}M_{\odot}$, and another five Milky Way-type halos (MW1-5) with $M \approx 10^{12}h^{-1}M_{\odot}$. The particulars of these hosts are summarised in Table 1.

For the interested reader, C1-8 have been generated with the adaptive mesh refinement code **MLAPM** (Knebe et al.

2001) and their properties have been discussed in detail in Warnick & Knebe (2006) and Warnick et al. (2008). MW1 corresponds to model “Box20” of Prada et al. (2006) that has been simulated with the **ART** code (Kravtsov et al. 1997). All other halos (i.e. MC1-3, C9-12, G1-5, MW2-5) have been simulated with the Tree-PM code **GADGET2** (Springel 2005) and their detailed properties will be presented in a forthcoming paper (Knollmann et al., in preparation). However, we wish to highlight that G1-G5 are drawn from a constrained realisation of the Local Universe (1024^3 particles in a box of side $64h^{-1}\text{Mpc}$; Yepes et al., in preparation).¹ MC1-3 are resimulations of individual halos embedded in a box of side $512h^{-1}\text{Mpc}$; MW2-4 are resimulations of individual halos embedded in a box of side $50h^{-1}\text{Mpc}$, while MW5 is a resimulation embedded in a box of side $150h^{-1}\text{Mpc}$.

Note that MC1-3, C9-12 and G1-5 have been simulated assuming a WMAP3 cosmology (Spergel et al. 2007), while all other systems were simulated assuming a WMAP1 cosmology (Spergel et al. 2003).

2.2 The Subhalos

Both host halos and subhalos are identified using **AHF**² (Knollmann et al., in preparation), an MPI parallelised modification of the **MHF**³ algorithm presented in Gill et al. (2004). **AHF** utilises an adaptive grid hierarchy to locate halos (subhalos) as peaks in an adaptively smoothed density field. Local potential minima are computed for each peak and the set of particles that are gravitationally bound to the peak are returned. If the peak contains in excess of 20 particles, then it is considered a halo (subhalo) and retained for further analysis.

For each halo (subhalo) we calculate a suite of canonical properties from particles within the virial (truncation) radius. We define the virial radius R_{vir} as the point at which the density profile (measured in terms of the cosmological background density ρ_b) drops below the virial overdensity Δ_{vir} , i.e. $M(< R_{\text{vir}})/(4\pi R_{\text{vir}}^3/3) = \Delta_{\text{vir}}\rho_b$.⁴ This prescription is not appropriate for subhalos in the dense environs of their host halo, where the local density exceeds $\Delta_{\text{vir}}\rho_b$, and so the density profile will show a characteristic upturn at a radius $R \lesssim R_{\text{vir}}$. In this case we use the radius at which the density profile shows this upturn to define the truncation radius for the subhalo. Further details of this approach can be found in Gill et al. (2004).

3 SUBHALO SHAPES

A generic prediction of the CDM model is that dark matter halos are triaxial systems, that can be reasonably approximated as ellipsoids (e.g. Frenk et al. 1988; Warren et al.

¹ See Klypin et al. (2003) for a presentation of the method applied to run constrained simulations.

² **AMIGA’s-Halo-Finder**; **AHF** can be downloaded from <http://www.aip.de/People/aknebe/AMIGA>. **AMIGA** is the successor to **MLAPM**.

³ **MLAPM’s-Halo-Finder**

⁴ For a distinct (i.e. host) halo in a ΛCDM cosmology with the cosmological parameters that we have adopted, $\Delta_{\text{vir}} = 340$ at $z = 0$.

1992; Kasun & Evrard 2005; Bailin & Steinmetz 2005; Allgood et al. 2006; Macciò et al. 2007; Bett et al. 2007; Gottlöber & Yepes 2007). Following others (e.g. Gerhard 1983; Bailin & Steinmetz 2005; Allgood et al. 2006; Pereira et al. 2007; Kuhlen et al. 2007; Faltenbacher et al. 2007), we measure the shape of the halos by the weighted moment of inertia:

$$I_{ij} = \sum_k m_k \frac{r_{ki} r_{kj}}{r_k^2}. \quad (1)$$

The axis ratios b/a and c/a are the square roots of the eigenvalues ($a > b > c$) and the corresponding eigenvectors $\mathbf{E}_a, \mathbf{E}_b, \mathbf{E}_c$ give the directions of the principal axes.

We wish to measure the direction of a subhalo’s principal axes with respect to the centre of the host, and so it is important to measure reliably shape and orientation. Therefore we follow Pereira et al. (2007) and require subhalos to contain at least $N_{p,\min} = 200$ for reliable shape estimation in this Section, and to have an axis ratio $b/a < 0.9$ when investigating the radial alignments in Section 4.

The numbers of subhalos in each host halo compliant with either of these two criteria are given in Table 1. One observes that there exists a prominent population of subhalos with $b/a > 0.9$. Careful inspection reveals that the distribution of $P(b/a)$ (not shown here) is Gaussian with the peak at about 0.89. This means that there is a substantial number of objects orbiting within the virial radius of the host which do not enter into our radial alignment analysis below. However, as also noted by Pereira et al. (2007), we confirm that the majority of these systems is spherical and hence a major axes cannot be robustly defined.⁵

Because we are interested in the dependence of both the shape and the radial alignment on the mass of the host, we stack data accordingly. All subhalos for MC, C, G, and MW hosts are combined into one single plot and hence there appear four panels in subsequent plots, one for each host class.

3.1 Shape Measurements

Triaxiality Using the eigenvalues $a > b > c$ of the moment of inertia tensor we calculate the triaxiality parameter (e.g. Franx et al. 1991)

$$T = \frac{a^2 - b^2}{a^2 - c^2}. \quad (2)$$

In Figure 1 we show the triaxiality probability distribution (solid histograms showing the fraction of subhalos in the respective bin and normalized to unity) for subhalos containing more than 200 particles; error bars assume Poisson errors. We further fitted a Gaussian to $P(T)$ and list the two fitting parameters (width σ and peak T_{peak}) in Table 2.

Sphericity Although triaxiality is useful for distinguishing prolate from oblate halos, we seek a more reliable measure for deviation from sphericity. We use the axis ratio

$$s = \frac{c}{a} \quad (3)$$

⁵ If we nevertheless include objects with $b/a \geq 0.9$ in the radial alignment analysis the signal is practically unaffected.

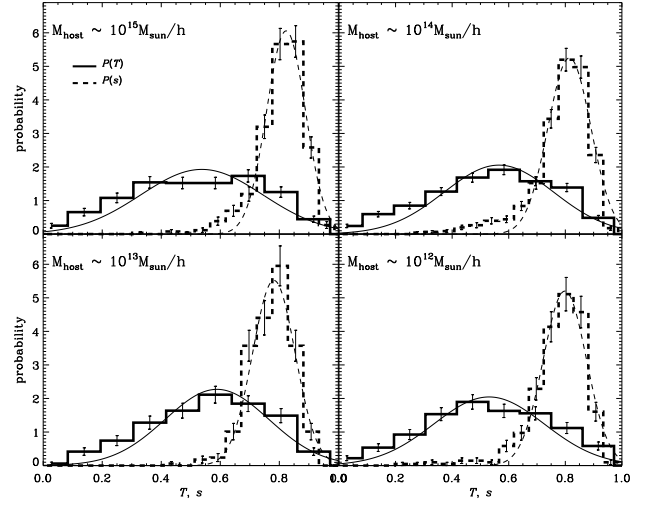


Figure 1. Distribution of subhalo triaxialities and subhalo shapes. Only subhalos with more than $N_p > 200$ are considered.

Table 2. Gaussian’s parameters for the probability distribution of triaxiality and sphericity.

| host | $P(T)$ | | $P(s)$ | |
|------|-------------------|----------|-------------------|----------|
| | T_{peak} | σ | s_{peak} | σ |
| MC | 0.54 | 0.21 | 0.82 | 0.07 |
| C | 0.57 | 0.19 | 0.81 | 0.08 |
| G | 0.59 | 0.18 | 0.78 | 0.07 |
| MW | 0.53 | 0.20 | 0.80 | 0.08 |

for this purpose; a spherical halo has $c/a \rightarrow 1$ while a highly oblate or prolate halo has $c/a \rightarrow 0$. The resulting distributions for subhalos in excess of 200 particles can be viewed in Figure 1 (dashed histograms), too. The corresponding best-fit parameters of a Gaussian are again listed in Table 2.

3.2 Discussion

There is an extensive literature on the shape of isolated/field dark matter halos (e.g. Frenk et al. 1988; Warren et al. 1992; Kasun & Evrard 2005; Bailin & Steinmetz 2005; Allgood et al. 2006; Macciò et al. 2007; Bett et al. 2007). These studies indicate that the average triaxiality and sphericity of isolated halos is $\langle T \rangle \approx 0.75$ and $\langle s \rangle \approx 0.66$, respectively.

The first extension of such studies to subhalo populations was presented by Kuhlen et al. (2007) for the “Via Lactea” simulation (Diemand et al. 2007), an ultra-high resolution simulation of a Milky Way-type dark matter halo. We do not have the resolution of the Via Lactea simulation but we do have a statistical sample of sufficiently well resolved systems to explore the shapes of subhalos.

In agreement with Kuhlen et al. (2007), we observe that subhalos are triaxial with $\langle T \rangle \approx 0.55$ (cf. Table 2), irrespective of the host mass. We note also that the distribution of T as presented in Figure 1 (solid histograms) is well fitted by a Gaussian. The same holds for the distribution of sphericities $P(s)$ presented in Figure 1 (dashed histograms), too (cf. also Fig.3 in Faltenbacher et al. (2007)). However,

our sphericities are typically $\langle s \rangle \approx 0.80$ and are marginally larger than the ones reported by Kuhlen et al. (2007) and Faltenbacher et al. (2007) ($\langle s \rangle \approx 0.74$). This likely reflects the different halo finding algorithms; both Kuhlen et al. (2007) and Faltenbacher et al. (2007) use a method derived from the friends-of-friends algorithm, whereas we use a spherical halo finder AHF (cf. Gill et al. (2004) who performed an in-depth comparison of AHF, FOF and SKID.)

4 SUBHALO ALIGNMENTS

The principal aim of this study is to investigate whether or not there is a dependence of the radial alignment of subhalos (i.e. the alignment of their major axis with respect to the centre of the host) on the mass of their host halo. Recent observational evidence suggests that the major axis (in projection) of satellite galaxies tend to “point towards the centre of their host” (e.g. Pereira & Kuhn 2005; Agustsson & Brainerd 2006; Yang et al. 2006; Faltenbacher et al. 2007; Wang et al. 2007). It is therefore natural to ask whether or not subhalos in cosmological simulations display a similar trend. To date a few studies have investigated this subject (Kuhlen et al. 2007; Faltenbacher et al. 2007; Pereira et al. 2007). We extend this work by examining the mass dependence of the radial alignment.

4.1 Measurement of Radial Alignment

To measure the radial alignment of subhalos, we use the eigenvector \mathbf{E}_a which corresponds to the direction of the major axis a of the subhalo. We quantify the radial alignment of subhalos as the angle between the major axis E_a of each subhalo and the radius vector of the subhalo in the reference frame of the host:

$$\cos \theta = \frac{\mathbf{R}_{\text{sub}} \cdot \mathbf{E}_{a,\text{sub}}}{|\mathbf{R}_{\text{sub}}| |\mathbf{E}_{a,\text{sub}}|} \quad (4)$$

The (normalized) distribution $P(\cos \theta)$ of $\cos \theta$ measuring the fraction of subhaloes in the respective bin can be viewed in Figure 2.

We find a positive radial alignment signal different from isotropy, in agreement with Kuhlen et al. (2007), Faltenbacher et al. (2007) and Pereira et al. (2007). This can be verified in Table 3 where we compare the cumulative probability distributions $P(< \cos \theta)$ (shown as thin solid lines in Figure 2, too) with the isotropic distribution by applying a Kolmogorov-Smirnov (KS) test. The resulting KS probabilities are consistent with zero. They are listed in Table 3 alongside D , the maximum distance of the actual and isotropic distribution.

To better quantify these differences, we fit the following heuristically determined function to the (differential) probability distributions

$$P(x) = \left(\frac{1}{B + A/5} \right) A x^4 + B, \quad (5)$$

with $x = \cos \theta$. In order to gauge the error introduced by binning the data we perform the fit to differently binned $P(\cos \theta)$ changing N_{bins} steadily from 5 to 15; $\langle A \rangle$ and $\langle B \rangle$

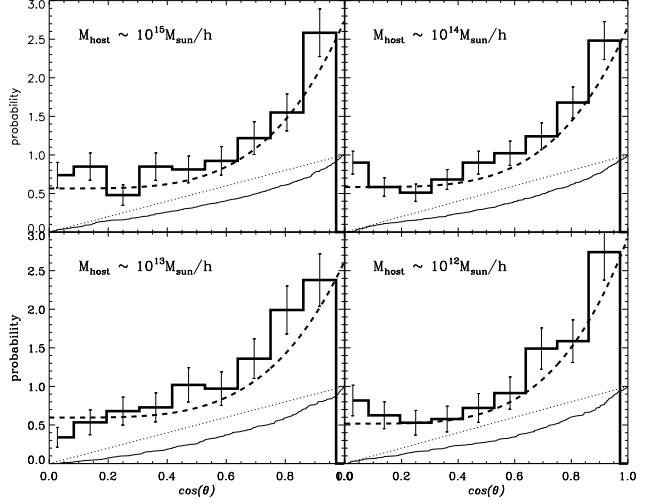


Figure 2. Distribution of subhalo radial alignment. The histograms are the differential distribution (with Poissonian error bars) that have been fitted by Eq. (5) (dashed line). The continuous line represents the cumulative probability distribution $P(< \cos \theta)$; the dotted line is the (cumulative) isotropic distribution. Only subhalos with $N_p > 200$ and $b/a < 0.9$ are considered.

Table 3. Kolmogorov-Smirnov test and best fit parameters for radial alignment probability distribution. The errors for A and B are based upon fitting Eq. (5) to $P(\cos \theta)$ using different number of bins $N_{\text{bins}} \in [5, 15]$ and $\langle A \rangle$ and $\langle B \rangle$ are the respective mean values.

| host | D | KS probability | $\langle A \rangle$ | $\langle B \rangle$ |
|------|-------|---------------------|---------------------|---------------------|
| MC | 0.266 | 6×10^{-09} | 2.81 ± 0.22 | 0.56 ± 0.05 |
| C | 0.262 | 6×10^{-13} | 2.67 ± 0.23 | 0.60 ± 0.05 |
| G | 0.306 | 5×10^{-09} | 2.50 ± 0.25 | 0.60 ± 0.04 |
| MW | 0.327 | 3×10^{-10} | 2.58 ± 0.26 | 0.58 ± 0.04 |

given in Table 3 are the corresponding means of the best-fit parameters and the errors are the 1σ -deviation. We note that these values are practically identical across hosts and do not depend on mass. This suggests that there is no (hidden or obvious) relation between the radial alignment of the subhalos and the mass of the host. This implies that any explanation of this phenomenon has to apply to galactic halos as well as clusters of mass $10^{15} h^{-1} M_{\odot}$.

4.2 Discussion

Both Yang et al. (2006) and Wang et al. (2007) report that the spatial anisotropy of satellite galaxies depends on host halo mass. In contrast, no such mass dependence has been reported for the radial alignment of satellite galaxies with respect to the host. This can be understood if one considers the physical origin of these effects. The spatial anisotropy is linked to the anisotropic infall of subhalos (and presumably satellite galaxies) onto their host halo (e.g. Knebe et al. 2004), and so can be considered an environmental effect. In contrast, the radial alignment is a dynamical effect (Kuhlen et al. 2007; Pereira et al. 2007), driven by the tidal field of the host halo (Ciotti & Dutta

1994); the subhalo adjusts its orientation in response to the tidal field on a timescale that is much shorter than the Hubble time. However, it is difficult to determine whether or not a subhalo adjusts its orientation by rigid body rotation (e.g. Kuhlen et al. 2007; Pereira et al. 2007) or by changing its shape; it is not straightforward to distinguish between changes in subhalo shape and “simple” figure rotation, especially for subhalos which are suffering mass loss. While the latter has been confirmed for isolated/host halos (Bailin & Steinmetz 2004) it has yet to be verified for subhalos.

5 SUMMARY AND CONCLUSIONS

We have examined the whether or not the radial alignment of the major axes of subhalos with respect to the centre of their host dark matter halo is dependent on host halo mass. Our results draw upon a sample of 25 cosmological high resolution resimulations of halos spanning galaxy- to cluster-mass scales ($10^{12} h^{-1} M_{\odot}$ to $10^{15} h^{-1} M_{\odot}$), the majority of them containing in excess of 10^6 particles within the virial radius. Our main results may be summarised as follows:

- Subhalos tend to be more spherical than isolated halos, with $\langle s \rangle \approx 0.80$.
- Subhalos have triaxialities $\langle T \rangle \approx 0.53$, lower than isolated halos.
- The probability distribution of $\cos \theta$ (i.e. the angle between the major axis \mathbf{E}_a of a subhalo and its radius vector in the reference frame of the host) can be well described by a simple power law $P(\cos \theta) \propto \cos^4 \theta$
- These results do not depend on the mass of the host system.

ACKNOWLEDGEMENTS

AK and ND acknowledge funding through the Emmy Noether programme of the DFG (KN 755/1). CP is supported by the STFC rolling grant for theoretical astrophysics at the University of Leicester. The numerical simulations of G1-5 and MW2-4 were performed at the LRZ Munich, NIC Jülich and BSC Barcelona. We thank DEISA for providing time to these computers under DECI project SIMU-LU. MC1-3, C1-12, and MW5 were carried out on Swinburne University’s supercomputer. The analysis was partly performed on the Sanssouci cluster of the AIP and at the LRZ Munich.

REFERENCES

- Adelman-McCarthy J. K. e. a., 2007, ApJS, 172, 634
 Agustsson I., Brainerd T. G., 2006, ApJ, 644, L25
 Allgood B., Flores R. A., Primack J. R., Kravtsov A. V., Wechsler R. H., Faltenbacher A., Bullock J. S., 2006, MNRAS, 367, 1781
 Bailin J., Power C., Norberg P., Zaritsky D., Gibson B. K., 2007, ArXiv e-prints, 706
 Bailin J., Steinmetz M., 2004, ApJ, 616, 27
 Bailin J., Steinmetz M., 2005, ApJ, 627, 647
 Bernstein G. M., Norberg P., 2002, AJ, 124, 733
 Bett P., Eke V., Frenk C. S., Jenkins A., Helly J., Navarro J., 2007, MNRAS, 376, 215
 Brainerd T. G., 2005, ApJ, 628, L101
 Ciotti L., Dutta S. N., 1994, MNRAS, 270, 390
 Colless M. e. a., 2003, ArXiv Astrophysics e-prints
 Diemand J., Kuhlen M., Madau P., 2007, ApJ, 657, 262
 Faltenbacher A., Jing Y. P., Li C., Mao S., Mo H. J., Pasquali A., van den Bosch F. C., 2007, ArXiv e-prints, 706
 Faltenbacher A., Li C., Mao S., van den Bosch F. C., Yang X., Jing Y. P., Pasquali A., Mo H. J., 2007, ApJ, 662, L71
 Franx M., Illingworth G., de Zeeuw T., 1991, ApJ, 383, 112
 Freeman K., Bland-Hawthorn J., 2002, ARA&A, 40, 487
 Frenk C. S., White S. D. M., Davis M., Efstathiou G., 1988, ApJ, 327, 507
 Gerhard O. E., 1983, MNRAS, 202, 1159
 Gill S. P. D., Knebe A., Gibson B. K., 2004, MNRAS, 351, 399
 Gottlöber S., Yepes G., 2007, ApJ, 664, 117
 Hawley D. L., Peebles P. J. E., 1975, AJ, 80, 477
 Kasun S. F., Evrard A. E., 2005, ApJ, 629, 781
 Klypin A., Gottlöber S., Kravtsov A. V., Khokhlov A. M., 1999, ApJ, 516, 530
 Klypin A., Hoffman Y., Kravtsov A. V., Gottlöber S., 2003, ApJ, 596, 19
 Knebe A., Gill S. P. D., Gibson B. K., Lewis G. F., Ibata R. A., Dopita M. A., 2004, ApJ, 603, 7
 Knebe A., Green A., Binney J., 2001, MNRAS, 325, 845
 Kravtsov A. V., Klypin A. A., Khokhlov A. M., 1997, ApJS, 111, 73
 Kuhlen M., Diemand J., Madau P., 2007, ApJ, 671, 1135
 Lee J., Kang X., Jing Y. P., 2005, ApJ, 629, L5
 Libeskind N. I., Frenk C. S., Cole S., Helly J. C., Jenkins A., Navarro J. F., Power C., 2005, MNRAS, 363, 146
 Macciò A. V., Dutton A. A., van den Bosch F. C., Moore B., Potter D., Stadel J., 2007, MNRAS, 378, 55
 Pereira M. J., Bryan G. L., Gill S. P. D., 2007, ArXiv e-prints, 707
 Pereira M. J., Kuhn J. R., 2005, ApJ, 627, L21
 Prada F., Klypin A. A., Simonneau E., Betancort-Rijo J., Patiri S., Gottlöber S., Sanchez-Conde M. A., 2006, ApJ, 645, 1001
 Sales L., Lambas D. G., 2004, MNRAS, 348, 1236
 Spergel et al. D. N., 2003, ApJS, 148, 175
 Spergel et al. D. N., 2007, ApJS, 170, 377
 Springel V., 2005, MNRAS, 364, 1105
 Thompson L. A., 1976, ApJ, 209, 22
 Wang Y., Yang X., Mo H. J., Li C., van den Bosch F. C., Fan Z., Chen X., 2007, ArXiv e-prints, 710
 Warnick K., Knebe A., 2006, MNRAS, 369, 1253
 Warnick K., Knebe A., Power C., 2008, MNRAS, 389, 999
 Warren M. S., Quinn P. J., Salmon J. K., Zurek W. H., 1992, ApJ, 399, 405
 Yang X., van den Bosch F. C., Mo H. J., Mao S., Kang X., Weinmann S. M., Guo Y., Jing Y. P., 2006, MNRAS, 369, 1293
 Zaritsky D., Smith R., Frenk C. S., White S. D. M., 1997, ApJ, 478, L53+
 Zentner A. R., Kravtsov A. V., Gnedin O. Y., Klypin A. A., 2005, ApJ, 629, 219

This paper has been typeset from a \TeX / \LaTeX file prepared by the author.